J Mater Sci: Mater Med (2015) 26:274
DOI 10.1007/s10856-015-5599-8

BIOCOMPATIBILITY STUDIES

Original Research

Biomineralization and biocompatibility studies of bone conductive scaffolds containing poly(3,4-ethylenedioxythiophene): poly(4-styrene sulfonate) (PEDOT:PSS)

Mostafa Yazdimamaghani[1,2] · Mehdi Razavi[1,3,4] · Masoud Mozafari[1,5] · Daryoosh Vashaee[6] · Hari Kotturi[7] · Lobat Tayebi[1,8,9]

Received: 9 July 2015 / Accepted: 3 October 2015 / Published online: 5 November 2015

Abstract Considering the well-known phenomenon of enhancing bone healing by applying electromagnetic stimulation, manufacturing conductive bone scaffolds is on demand to facilitate the delivery of electromagnetic stimulation to the injured region, which in turn significantly expedites the healing procedure in tissue engineering methods. For this purpose, hybrid conductive scaffolds composed of poly(3,4-ethylenedioxythiophene), poly(4-styrene sulfonate) (PEDOT:PSS), gelatin (Gel), and bioactive glass (BaG) were produced employing freeze drying technique. Concentration of PEDOT:PSS were optimized to design the most appropriate conductive scaffold in terms of biocompatibility and cell proliferation. More specifically, scaffolds with four different compositions of 0, 0.1, 0.3 and 0.6 % (w/w) PEDOT:PSS in the mixture of 10 % (w/v) Gel and 30 % (w/v) BaG were synthesized. Immersing the scaffolds in simulated body fluid (SBF), we evaluated the bioactivity of samples, and the biomineralization were studied in details using scanning electron microscopy, energy dispersive spectroscopy, X-ray diffraction analysis and Fourier transform infrared spectroscopy. By performing cytocompatibility analyses for 21 days using adult human mesenchymal stem cells, we concluded that the scaffolds with 0.3 % (w/w) PEDOT:PSS and conductivity of 170 μS/m has the optimized composition and further increasing the PEDOT:PSS content has inverse effect on cell proliferation. Based on our finding, addition of this optimized amount of PEDOT:PSS to our composition can increase the cell viability more than 4 times compared to a nonconductive composition.

Mostafa Yazdimamaghani and Mehdi Razavi contributed equally to this work.

✉ Lobat Tayebi
lobat.tayebi@marquette.edu

[1] Helmerich Advanced Technology Research Center, Oklahoma State University, Tulsa, OK 74106, USA

[2] School of Chemical Engineering, Oklahoma State University, Stillwater, OK 74078, USA

[3] BCAST, Institute of Materials and Manufacturing, Brunel University London, Uxbridge, London UB8 3PH, UK

[4] Brunel Institute for Bioengineering, Brunel University London, Uxbridge, London UB8 3PH, UK

[5] Bioengineering Research Group, Nanotechnology and Advanced Materials Department, Materials and Energy Research Center (MERC), P.O. Box 14155-4777, Tehran, Iran

[6] Electrical and Computer Engineering Department, North Carolina State University, Raleigh, NC 27606, USA

[7] Department of Biology, University of Central Oklahoma, Edmond, OK 73034, USA

[8] Biomaterials and Advanced Drug Delivery Laboratory, Stanford University, Palo Alto, CA 94305, USA

[9] Department of Developmental Sciences, Marquette University School of Dentistry, Milwaukee, WI 53233, USA

1 Introduction

Ongoing studies in tissue engineering scaffold design are mostly focused on improving the physical characteristics of the scaffolds with respect to their chemical and mechanical properties [1–4]. However, electrical properties of such scaffolds have not been widely studied [5–7]. The conductivity of scaffolds has two important effects: (a) it will enhance the signaling among the cells, and (b) allows the local delivery of external electrical stimuli to the site of defects to enhance the healing procedure. However, there

are few studies that investigated the effect of the conductive polymers in cell signaling, enhancement of cell proliferation and their application in the tissue engineering field, which is the subject of our study in this paper [8–12].

There is a large discrepancy in the literature regarding the quantitative values presented for the electrical properties of bone and other biological tissues. This is due to the different fluid content of tissues examined from different parts of the body by different researchers, absence of standardized methods of measurement, and different age and health situation of the obtained tissues. In addition, the anisotropic property of the bone can induce electrical anisotropy, and thus the orientation of the bone in the measurements must be considered in comparing different reported data. Moreover, perfect alignment of the anisotropic tissue is essential in the measurement techniques since a slight misalignment can bring about 20 % overestimation to data. Fluid content of the biological tissue induce a drastic difference in their electric properties. The conductivity of the brain and blood is considered to be relatively high, however, fat, skin and bone has lower conductivity due to less fluid content in the range of $10–10^4$ μS/m [13]. Experiments indicate scaffolds with conductivity values of more than 10^2 μS/m can effectively increase cell proliferation and hence improve healing process in bone tissue engineering applications [9].

Among water-soluble conductive polymers, poly(3,4-ethylenedioxythiophene) (PEDOT) has been known as a promising one. Due to its biocompatibility and similarity with natural biological materials like melanin, PEDOT has also been introduced as a biomaterial in some studies [8, 14–17]. Poly(sodium 4-styrene-sulfonate) (PSS) is another water-soluble polymer. Investigations have demonstrated that sulfonic groups on the polymer surfaces enhance the cell attachment. The characteristics of both PEDOT and PSS make the combination of PEDOT:PSS a good candidate to be utilized as a conductive polymer with high ductility in different applications [16, 18–21]. Gelatin (Gel), as a natural biopolymer, has been broadly used in the pharmaceutical and medical applications because of its biological source, degradability, biocompatibility, availability, and relatively low cost [22–24]. As a bioactive ceramic, bioactive glasses (BaG) have indicated outstanding integration to the hard tissue due to the precipitation of calcium phosphate minerals on the BaG surface in the physiological environment [25].

According to the aforementioned advantages of these components, we have previously produced macroporous 3 dimensional (3D) hybrid scaffolds composed of PEDOT, Gel, and bioactive glass [9]. Material characterizations, in vitro scaffold swelling and degradation, thermal and mechanical analysis investigation on scaffolds were performed. Addition of PEDOT:PSS not only made a conductive construct but significantly enhanced our mechanical properties. Increase of cell viability was observed by increase of PEDOT:PSS content and we discussed in detail how the incorporation of a suitable conductive polymer could increase the cell signaling and consequently improve the cell viability on the scaffolds. In this paper we will show that there is an optimized value for the amount of PEDOT:PSS in our composition to be able to gain its positive possession, and the excess of this polymer can cause cytotoxicity. Therefore, in this study several compositions with different concentrations of PEDOT were prepared and characterized in order to optimize the amount of PEDOT:PSS. To obtain a better cytocompatibility and cell viability overview, adult human mesenchymal stem cells (hMSC) were cultured on the scaffolds for 21 days and morphology, cell contact, attachment and viability of the cells were studied. Moreover, biomineralization behavior of the synthesized scaffolds in simulated body fluid (SBF) was investigated in detail and evaluated by FTIR, scanning electron microscopy (SEM) and EDX. These experiments offer a solid view of mimicking bone generation and ability of the optimized scaffold to bind to the surrounding hard tissues. We believe that these conductive scaffolds provide excellent biocompatibility with appropriate properties, such as improved cell proliferation and adhesion, as well as enhanced mechanical properties.

2 Materials and methods

Synthesis of scaffolds: The initial precursors for synthesizing the scaffolds include PEDOT:PSS (1.3 wt % dispersion in water, PEDOT content 0.5 wt %, PSS content 0.8 wt %, conductive grade, Sigma Aldrich), Gelatin (from porcine skin, Type A, Sigma Aldrich), and 0.1 M HNO_3 (Sigma Aldrich), the crosslinker 1-(3-dimethylaminopropyl)-3-ethylcarbodiimide hydrochloride (Acros Organics, Geel, Belgium), *N*-hydroxysuccinimide ($C_4H_5NO_3$, Alfa Aesar, Ward Hill, MA, USA), and the 64S bioactive glass (BaG) which was produced in our lab using the previously reported sol–gel method [1, 26]. A solution composed of Gel (10 % w/v), BaG (30 % w/v), and PEDOT:PSS (0, 0.1, 0.3 and 0.6 % w/w) was prepared by dissolving 10 g Gel and 30 g BaG in 100 mL deionized water to make the initial Gel/BaG solution. Then, the PEDOT:PSS (0.1, 0.3 or 0.6 % w/w of the whole mass of the mixture) was added to this solution. The PEDOT:PSS/Gel/BaG solution was homogenized by utilizing a vortex for 5 min and a centrifugal mixer (Uni Cyclone UM113; Japan Unix Co., Tokyo, Japan) at 2000 rpm for half an hour. To produce the scaffolds employing the freeze-drying technique, the homogenized solution were molded and frozen at −20 °C for 6 h. The temperature, pressure, and

time set of the freeze-dryer (Labconco, Kansas City, MO, USA) were adjusted at −50 °C, 1.8 mbar and 24 h, respectively. The obtained porous materials were cross-linked using the 1-ethyl-3-(3-dimethylaminopropyl) carbodiimide hydrochloride (50 mM)/*N*-hydroxysuccinimide (8 mM)/ethanol (95 %) solution at 4 °C for 48 h.

Bioactivity evaluation: In order to evaluate the bioactivity of samples, the prepared scaffolds were incubated in the SBF. The Kokubo's protocol was employed for the SBF preparation by using NaCl, $NaHCO_3$, KCl, $K_2HPO_4 \cdot 3H_2O$, $MgCl_2 \cdot 6H_2O$, $CaCl_2$, Tris-buffer, and 1 N HCl as the precursors [27]. The SBF solution was prepared by dissolving abovementioned materials into the distilled water and buffering at pH = 7.4 with Tris- and HCl 1 N at 37 °C.

Structural characterization: The structural morphology of the scaffolds was characterized via a scanning electron microscope (SEM: Hitachi S-4800, Tokyo, Japan). The porosity of scaffolds was determined by the ethanol replacement technique. Fourier transform infrared spectroscopy (FTIR: Agilent Technologies, Santa Clara, CA, USA) was employed to investigate the functional group of samples. The phase analysis was carried out using an X-ray diffractometer (XRD: Bruker Corporation, Billerica, MA, USA).

Culture of Human Mesenchymal Stem Cells: Cytocompatibility experiments were performed using the adult human mesenchymal stem cells (hMSC). Mesenchymal stem cells isolated from human bone marrow were purchased from life technologies (StemPro® BM, Life Technologies). As per manufacture's recommendations, cells were cultured in Mesen PRO RS media in humidified atmosphere of 5 % CO_2 and maintained at 37 °C. We first subcultured the purchased cells which were in passage 4 in a 75 cm^2 flasks. After 3 days, they were relocated to new 75 cm^2 flasks at a concentration of 4000 cell/cm^2. Cell culture media was changed every two days. Flasks that were observed to be 80 % confluent were first washed in DPBS, trypsinized with TrypLE™ Select CTS™ reagent (Life Technologies) and washed again to be prepared for our experiments. Cells of passage 6 (P6) were used for all of our experiments.

Cell Viability Assay: We evaluated the cell proliferation on different scaffolds using PrestoBlue® Cell Viability Reagent (Life Technologies, USA). PrestoBlue® is a resazurin-based non-fluorescent reagent reduced by viable cells into fluorescent molecule resorufin. Scaffolds were first sterilized using the ultraviolet for 2 h and placed in 24-well low-attachment culture plates. Three samples were utilized for each experiment and the data were reported as mean ± standard deviation.

Scaffolds were soaked in 2 mL of growth medium for 2 h, and then each scaffold was seeded with 8×10^4 cells in 1 mL of the cell suspension. For cell attachment, seeded scaffolds were incubated with cell suspension overnight in a humidified atmosphere of 370 °C and 5 % CO_2. After incubation, scaffolds were washed twice with PBS to eliminate any unattached cells, and were then relocated into a new plate. The plates were incubated for 7, 14 and 21 days while the Mesen PRO RS media was replaced every 2 days. Scaffolds soaked in media without cells were used as controls. After completion of the incubation period (7, 14, or 21 days), 100 μL of the PrestoBlue reagent was added to each well, followed by an additional 2 h incubation. Using a pasture pipette, we mixed the contents of each well to have uniform distribution of color. About 200 μL of the solution was added into a 96-well plate and the fluorescence was determined with an emission and exitation wavelength of 560 and 590 nm, respectively, using a spectrophotometer. Total number of viable cells attached to the scaffold was calculated using a standard curve which was generated by aliquoting cells into a 96-well plate within the range of 10,000–200,000 cells/well. After an 8 h incubation, cell viability was measured using the above mentioned kit as per manufacturer's protocol. A standard curve was generated by plotting number of cells versus fluorescence.

DAPI Staining: Cells attached to scaffolds with intact nuclei were visualized using florescence microscopy. 4′6-diamidino-2-phenylindole (DAPI), is a commonly used fluorescent dye for staining double-stranded DNA. Cell seeded onto scaffolds were fixed in 4 % paraformaldheyde for 30 min, and were then permeabilized with 0.1 % Triton-X 100 for 15 min and after each step scaffolds were thoroughly rinsed with sterile PBS at room temperature. This was followed by 20 min incubation of sections in DAPI (200 ng/mL) prepared in PBS. After the incubation, samples were gently rinsed with PBS. The morphology of the cell nuclei was observed under fluorescence microscope (Nikon, USA) at excitation wavelength of 350 nm. Nuclei with normal phenotype were expected to appear glowing bright.

After 7, 14 and 21 days, cell-containing scaffolds were fixed in 3.7 % formaldehyde for 0.5 h at room temperature. SEM imaging was performed after dehydrating the samples using ethanol.

A 2100 Digital Multimeter (Keithley Instruments, Inc, Cleveland, OH, USA) was employed for the conductivity measurements. The cylindrical samples with the dimensions of 9 mm diameter and 1 mm thickness were used for this experiment.

The prepared scaffolds with 0, 0.1, 0.3 and 0.6 % w/w PEDOT:PSS in the mixture of 10 % w/v Gel and 30 % w/v BaG were labeled 0PED, 0.1PED, 0.3PED, and 0.6PED, respectively in the paper.

3 Results

The numerical results demonstrated that the conductivity enhanced with the addition of PEDOT:PSS to the BaG/Gel composite up to 170 μS/m for the 0.3PED scaffold. The conductivity of 0PED, 0.1PED, 0.3PED, and 0.6PED was 100, 120, 170 and 210 μS/m, respectively.

SEM observation from the top view in high and low magnification was carried out to study the three dimensional morphology of the scaffolds (Fig. 1). The observations showed an interconnected network of spherical pores with high porosity for 0PED (a, b, c), 0.1PED (d, e, f), 0.3PED (g, h, i), and 0.6PED (j, k, l) scaffolds. Higher concentration of PEDOT:PSS led to an increase of the pore size, as can be observed in Fig. 1. Quantitatively, the average pore size of the scaffolds was 150 μm for 0PED samples, which increased gradually to 300 μm for 0.6PED samples. The porosity percent was approximately 60 % with 1–3 % rise by increasing PEDOT:PSS in the composite.

To understand the influence of the chemical composition of scaffolds on the cell/scaffold interactions, we assessed cell viability, morphology, and cell adhesion during the predetermined times (7, 14, and 21 days) using human mesenchymal stem cells (hMSC). For this purpose, after the sterilization of substrates, they were placed in a multiwall plate; the cells were directly cultured on top of the scaffolds' surfaces. After 7, 14, and 21 days, viability of cells in different scaffolds was assessed following by SEM imaging of the cell loaded scaffolds in order to compare their spreading and attachment. The results of the number of viable cells after 7, 14, and 21 days incubation on the

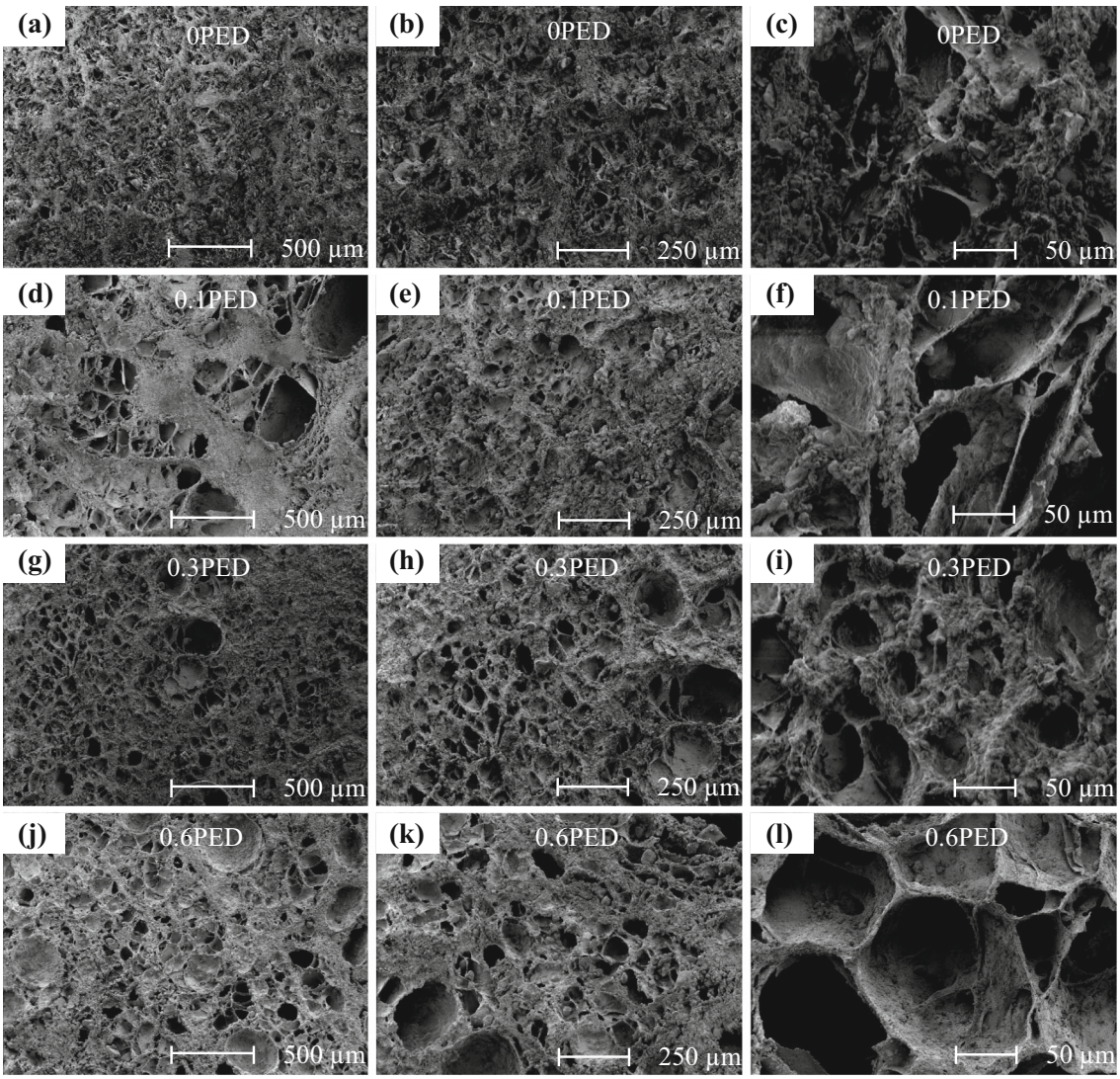

Fig. 1 SEM photomicrographs of 0PED (**a**, **b**, **c**), 0.1PED (**d**, **e**, **f**), 0.3PED (**g**, **h**, **i**), and 0.6PED (**j**, **k**, **l**) scaffolds in different magnifications showing the pores, pore sizes and the interconnectivity between the pores

0PED, 0.1PED, 0.3PED, and 0.6PED scaffolds have been presented in Fig. 2. According to this figure addition of PEDOT:PSS has significant positive influence on the viability of cells up to 0.3 % concentration. Increasing the amount of the PEDOT more than 0.3 % decreases the cell viability. A comparison between the viability of different scaffolds indicates that the number of viable cells on the 0.1PED and 0.3PED scaffold were almost similar with slightly better outcome in 0.3PED. To observe the cell morphology and attachment on scaffolds, SEM and confocal fluorescent microscopy were employed and examples are presented in Fig. 3. This figure displays the SEM images of the cells cultured for 14 days on the surfaces of scaffolds with different composition of PEDOT:PSS. As shown in these images, cell adhesion and response of the cells to the different surfaces were not similar. Repeating the experiment with various samples, we realized that cell attachment was noticeably improved in 0.3PED scaffolds. Figure 3e presents the fluorescent microscopy image of the 0.3PED scaffold after 14 days.

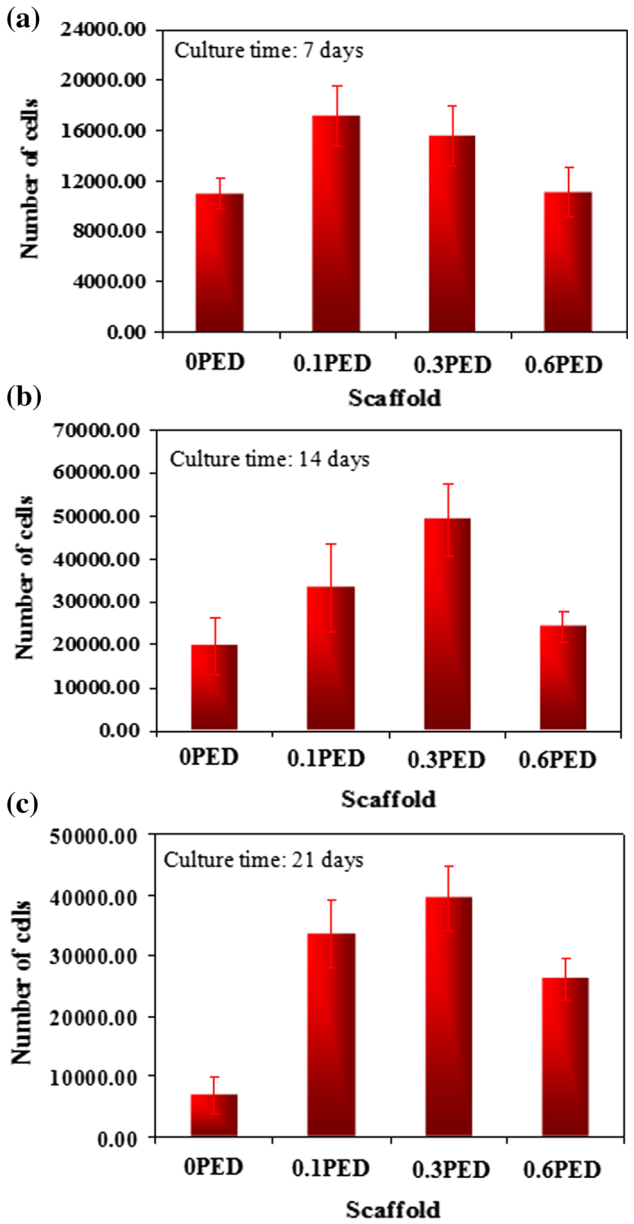

Fig. 2 The number of cells after 7, 14, and 21 days of incubation on the 0PED, 0.1PED, 0.3PED, and 0.6PED scaffolds

The quality of cell adhesion is known to greatly influence the proliferation and differentiation of cells. We observed better proliferation in 0.3PED scaffolds, in which cells reached to a confluent monolayer of cells on the surface. Figure 3 also shows the attached cells on the surface of the 0.3PED scaffold after 7 (f), 14 (g), and 21 (h, i) days. Accordingly, the cells on the 0.3PED scaffold exhibited stretched shapes during the cell culture times (7, 14, and 21 days). Cells showed numerous filopodia with anchorage points to the surface of the 0.3PED scaffold, denoting a favorable 3D structure and composition of conductive scaffolds for cell growth.

The samples were incubated into the SBF in order to follow their in vitro biomineralization. Figure 4 shows the SEM micrographs of 0.3PED scaffolds after 1 (a, c), and 14 (b, d) days immersion in the SBF. As indicated in Fig. 4b and d, a layer was found deposited on the surface. The precipitations appeared in ball-like structure (Fig. 4d). It can be observed in Fig. 4a that the scaffold surface morphology was degraded and a few cracks appeared on the surface.

Figure 5 shows the results of energy dispersive spectroscopy (EDS) (a, b, c, d, e) analyses and the related SEM micrographs (f, g, h, i, j) of the 0.3PED scaffold before (a, f) and after 1 (b, g), 3 (c, h), 7 (d, i) and 14 (e, j) day/days incubation in the SBF. According to Fig. 5a–e, Ca, P, and Si peaks could be detected in the EDS analyses. Prior to immersion in the SBF, the intensity of Si peak was higher than the intensity of Ca and P elements due to the existence of bioactive glass in the chemical composition of the scaffold. However, after the immersion in the SBF, the Si peak in EDS analyses was decreasing, whereas the intensity of Ca and P was in opposite trend by increasing the immersion time, showing that the Ca and P containing precipitates elements were depositing on the surface of the scaffolds. The SEM images shows that the density of precipitates was increasing by time and the related EDS analyses confirm this fact by presenting the increasing intensity of Ca and P. Figure 5 also shows the detailed analysis of the deposited layer on the surface of grinded 0.3PED scaffolds before and after 1, 3, 7, and 14 day/days immersion in the SBF, including FTIR (k) and X-ray diffraction analysis (XRD) (l) results. According to FTIR analysis, which has been presented in Fig. 5k, compared with scaffolds before immersion, the peaks corresponding

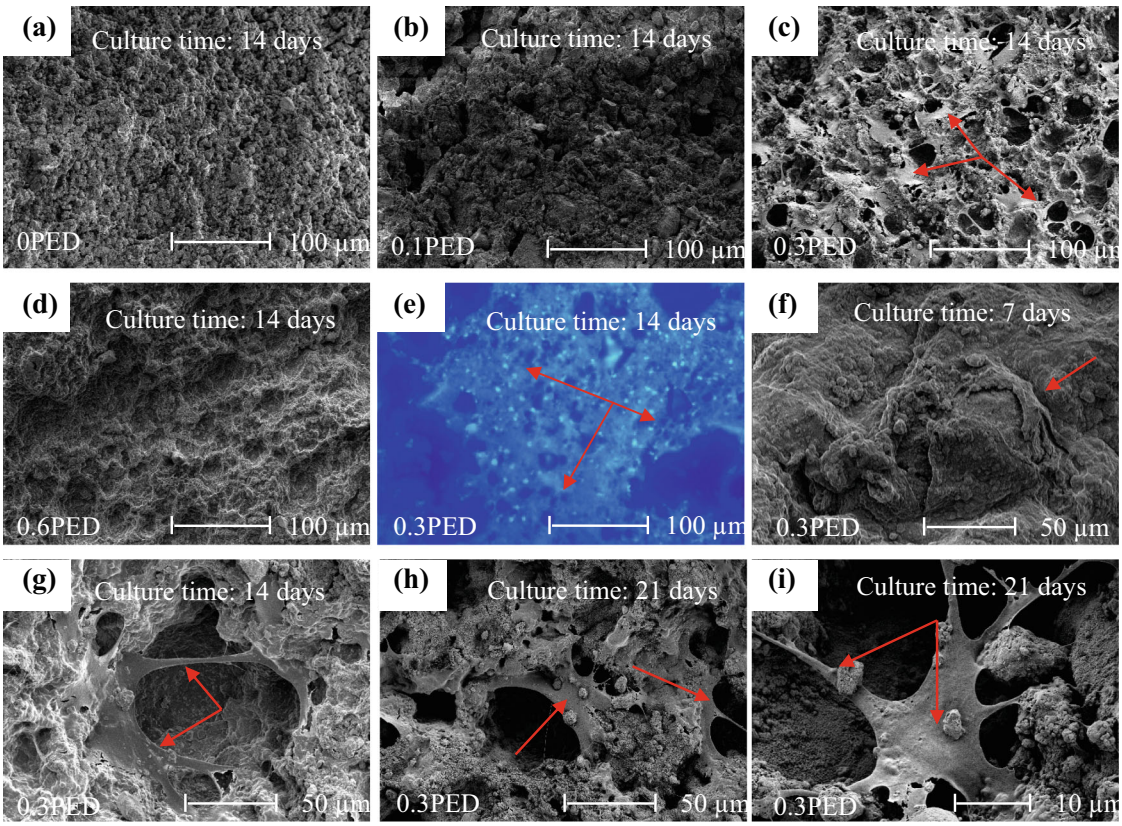

Fig. 3 SEM morphology of the cells cultured for 14 days on the surfaces of the 0PED (**a**), 0.1PED (**b**), 0.3PED (**c**), and 0.6PED (**d**) scaffolds, the fluorescent microscopy image from the 0.3PED scaffold after 14 days (**e**), the attached cells on the surface of 0.3PED scaffold after 7 (**f**), 14 (**g**), and 21 (**h**, **i**) days

to PO_4^{3-} groups have appeared on the surface after immersion, which increased by increasing the immersion time. This gradual rise of the intensity indicates the continuous apatite formation on the surface of immersed scaffolds. Appeared peaks at 601 cm^{-1} and 560 cm^{-1} are related to v_4 PO_4^{3-} vibrations and bands at 1036 cm^{-1} raised from v_3 PO_4^{3-} vibrations. The XRD patterns, according to Fig. 5l, confirm that a reaction layer composed of bone-like apatite has been precipitated on the surface of 0.3PED scaffolds. In early days of immersion, new peaks at 2θ of 26° and 31.7° related to (0 0 2) and (2 1 1) lattice planes of apatite phase according to the standard JCPDS file No. 090432 were observed. With prolongation of mineralization time, these two peaks were intensified and two other peaks of apatite were also found at 27.5°, 39.7° and 46.7°.

4 Discussion

The conductivity of produced BaG/Gel/PEDOT:PSS scaffolds was measured. The increase in the conductivity can be a result of the charge carrier (hole) motion in the PEDOT:PSS grains that are dispersed in the structure of the conductive scaffolds [9]. Scaffolds with 150–300 µm pore size and 60 % porosity can provide a suitable surface area for cell growth, sufficient volume for cell mass, and an easy platform for the transfer of the nutrition and removal of the waste from the cell growth sites. Appropriate size of the pores and their interconnectivity can enhance the metabolic activity of cells by the facilitating the diffusion of nutrients inside the scaffold and metabolic wastes out of it. The osteoblast ingrowth to the scaffold with appropriate pore size has positive influence on the mechanical bonding between the natural bone and the scaffold. This bonding leads to biological fixation of the scaffold in the nonunion part of the fracture and ultimate biodegradation and replacement with the host bone [9, 28]. In tissue engineering methods, cells are seeded in a 3D scaffold which not only provides the anchorage for cell adhesion, but also provides suitable cellular environment that regulate cell differentiation, metabolic activity, and cell–cell signaling [29, 30]. Although the 0.1PED scaffold can present good cell adhesion, its quality increased by increasing the amount of the PEDOT to 0.3 %. However, the response of the cells does not improve by increasing the PEDOT:PSS

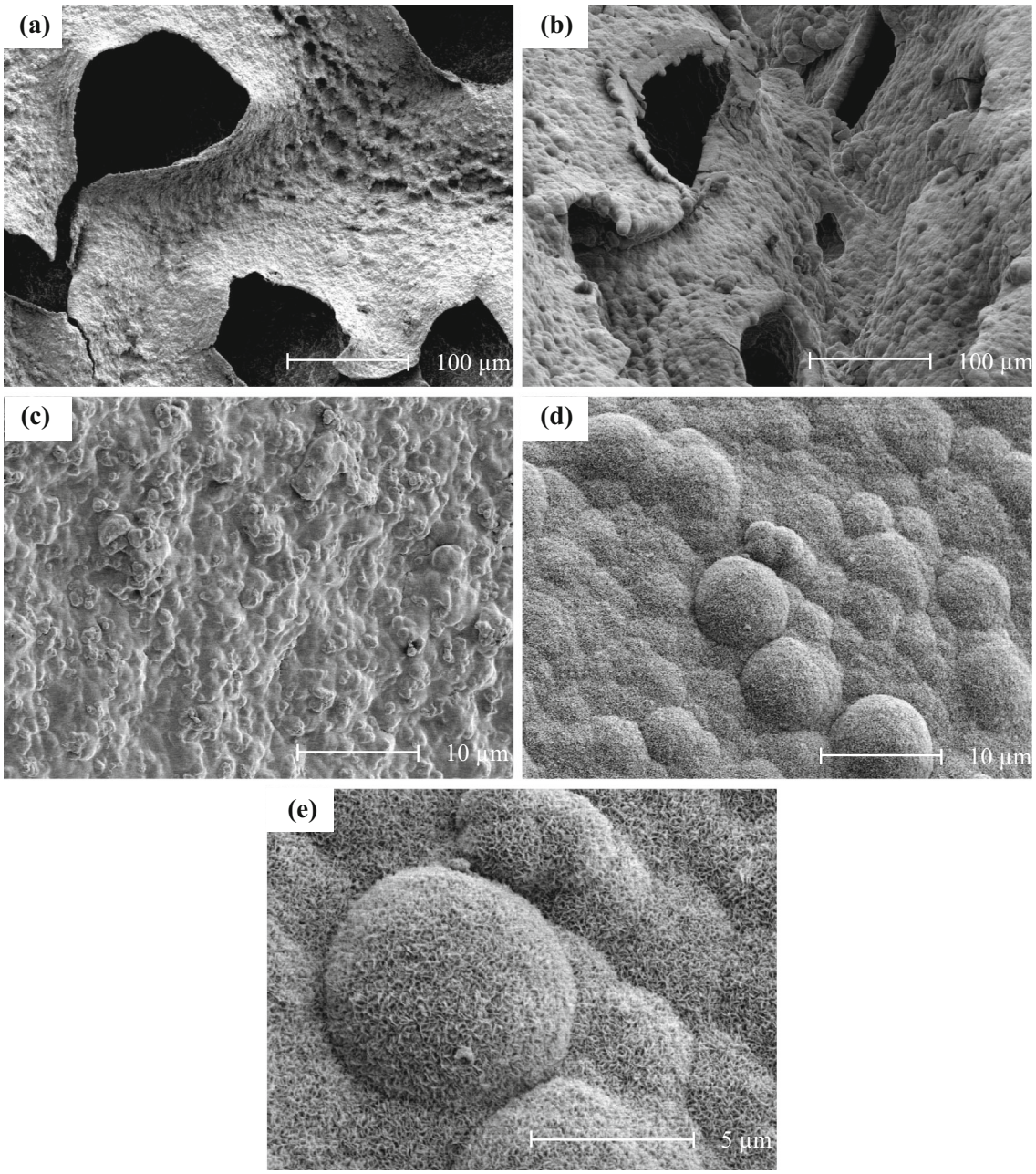

Fig. 4 SEM photomicrographs of 0.3PED scaffolds after 1 (**a**, **c**), and 14 (**b**, **d**) days immersion in the SBF

content over 0.3 % w/w (e.g., at 0.6PED scaffolds). The cells were more confluent and the area occupied by the cells increased on the surface of 0.3PED scaffolds compared to the others. The cells spread well and attached firmly on the surfaces of these scaffolds, indicating good cytocompatibility of 0.3PED samples. Considering the results of cell numbers (Fig. 2), cell attachments (Fig. 3) and repeating the experiments with different samples, we were convinced that 0.3 % is the most optimized concentration of PEDOT:PSS for our scaffolds in terms of the cell response and adhesion. Overall we concluded the enhanced cytocompatibility in 0.3PED compared to the other scaffolds, and accordingly, we performed the biomineralization experiments for the 0.3PED scaffold. Bioactivity is the ability of a biomaterial to encourage biological integration; and for hard tissue, bioactivity is related to the deposition of bioactive products, such as calcium phosphate apatite on the surface of samples in physiological environment [27, 31]. Regarding the comparison of the amount of deposited layer during the incubation time in the SBF solution, we realized that the deposited white layers on the surface of scaffolds were denser on the scaffold after 14 days. It can

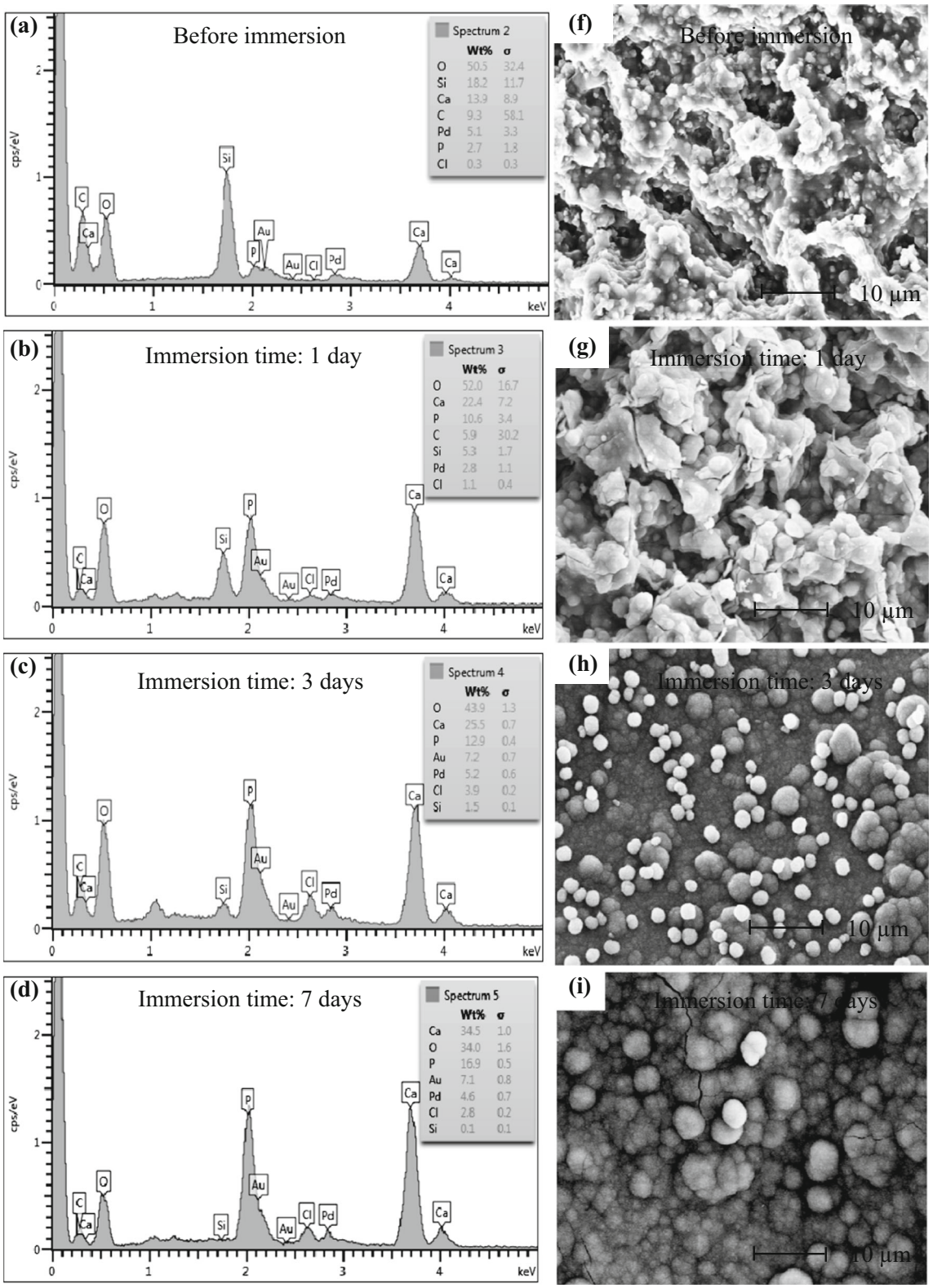

Fig. 5 The results of EDS (**a**, **b**, **c**, **d**, **e**) analysis and related SEM photomicrographs (**f**, **g**, **h**, **i**, **j**) from the 0.3PED scaffold before (**a**, **f**) and after 1 (**b**, **g**), 3 (**c**, **h**), 7 (**d**, **i**) and 14 (**e**, **j**) days incubation times in the SBF and the detailed analysis on the deposited layer on the surface of 0.3PED scaffold before and after 1, 3, 7, and 14 days immersion in the SBF including FTIR (**k**) and XRD (**l**) results

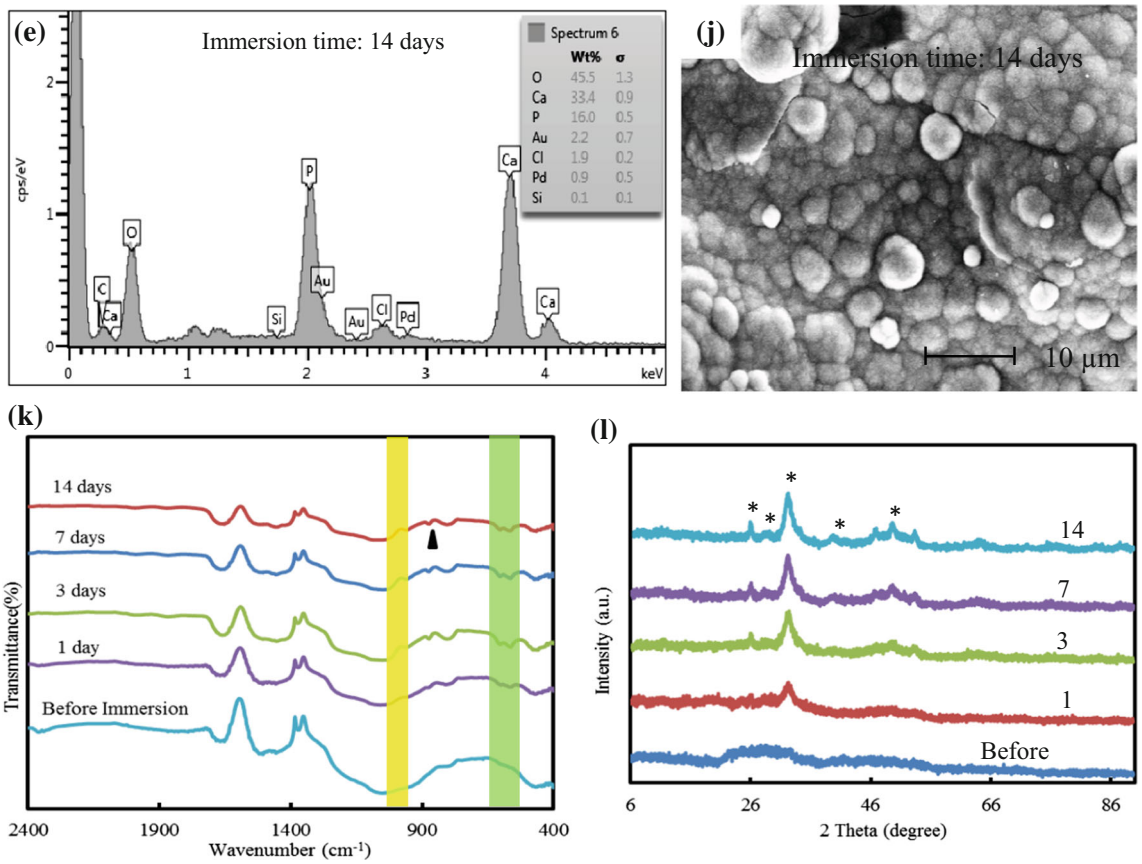

Fig. 5 continued

be concluded that the deposited layer on the surface nucleated and grew during the immersion time. Such bioactive minerals may be useful in enhancing the chances of osteointegrated interface formation between the scaffold and the host tissue after implantation [27, 32]. SBF is a supersaturated calcium phosphate solution and its chemical stimulus may activate the nucleation of bioactive minerals. The induction of bioactivity can be carried out by negatively charged groups. In particular, the formation of silanol (–Si–OH) on the surface of BaG particles is known to be beneficial for nucleation of bioactive products. These negatively charged groups attract Ca^{2+}, which in turn makes the positively charged sites for absorbing PO_4^{3-} and CO_3^{2-} in the SBF, which may eventually lead to the formation of a phosphate layer. Moreover, inorganic components of BaG, including calcium, phosphorous, and silicon which are bioactive minerals that exist in the inorganic structure of natural bone, are osteoproductive and osteoconductive. The glassy nature of BaG and its composition in the scaffolds are two crucial factors for bioactivity of this material. According to these factors and the proven glassy nature of the BaG using XRD, the scaffolds should bond to bone. When BaG composites are in contact with the body fluid, a layer of hydroxyapatite with incorporated collagen molecules forms on the surface which makes a biological bonding with the natural bone [25, 33]. Healing time is a prominent parameter in treatment of the large bone defects. When this time is extended, there is a risk of inappropriate connection of fractures. Due to the high demand for decreasing the healing time and enhancing its quality, several strategies have been developed, including employing electromagnetic stimuli [30, 34–40]. If the tissue engineering techniques are going to be combined with the strategy of applying electromagnetic stimuli, the scaffolds are needed to be conductive to locally deliver the stimuli to the site of the injury. Moreover, even without using electromagnetic stimulation, the conductivity of the scaffold assists electrical communication among cells. Since ion flux of cells influences the common cell behaviors, including cell attachment, viability, and migration, it is expected that applying conductive scaffolds effects overall cell response and viability [41, 42]. The reproducible observation of increased cell viability and proliferation in 0.3PED scaffolds might be the result of improved intracellular electrical cell signaling, which is essential for cell growth.

5 Conclusion

The purpose of this work was to construct an optimized conductive bone scaffold composed of PEDOT:PSS. The ultimate goal is applying effectual electromagnetic stimuli during the bone healing using degradable tissue engineering scaffolds. As the primary step to reach this aim, the authors prepared the conductive scaffolds by including PEDOT:PSS in the composition of BaG/Gel scaffolds. Characterizations of the scaffolds showed that they have porous structure with 60 % porosity and pore size of 150–300 μm. It was understood that the addition of PEDOT:PSS can improve various characteristics of the scaffolds, including biomineralization and biocompatibility. The optimum scaffold (0.3PED) with 0.3 % (w/w) PEDOT:PSS in the mixture of 10 % (w/v) Gel and 30 % (w/v) BaG (0.3PED scaffold) presented more cytocompatibility compared to others. The results of bioactivity revealed that the bone-like apatite was deposited on the surface of the 0.3PED scaffold, and the amount and density of bioactive products were increased by increasing the incubation time in the SBF. Our future work is focused on applying the electromagnetic stimulation both in vitro and in vivo to observe the effect of the stimulation on the growth of the cell on the synthesized conductive scaffold and ultimately on the bone healing.

References

1. Yazdimamaghani M, Vashaee D, Assefa S, Walker K, Madihally S, Köhler G, et al. Hybrid macroporous gelatin/bioactive-glass/nanosilver scaffolds with controlled degradation behavior and antimicrobial activity for bone tissue engineering. J Biomed Nanotechnol. 2014;10:911–31.
2. Yazdimamaghani M, Razavi M, Vashaee D, Tayebi L. Microstructural and mechanical study of PCL coated Mg scaffolds. Surf Eng. 2014;30:920–926.
3. Razavi M, Fathi M, Savabi O, Beni BH, Vashaee D, Tayebi L. Surface microstructure and in vitro analysis of nanostructured akermanite ($Ca_2MgSi_2O_7$) coating on biodegradable magnesium alloy for biomedical applications. Colloids Surf B. 2014;117:432–40.
4. Razavi M, Fathi MH, Savabi O, Vashaee D, Tayebi L. Biodegradation, bioactivity and in vivo biocompatibility analysis of plasma electrolytic oxidized (PEO) biodegradable Mg implants. Phys Sci Int J. 2014;4:708.
5. Bendrea AD, Cianga L, Cianga I. Review paper: progress in the field of conducting polymers for tissue engineering applications. J Biomater Appl. 2011;26:3–84.
6. De Giglio E, Sabbatini L, Colucci S, Zambonin G. Synthesis, analytical characterization, and osteoblast adhesion properties on RGD-grafted polypyrrole coatings on titanium substrates. J Biomater Sci-Polym Ed. 2000;11:1073–83.
7. Mozafari M, Salahinejad E, Shabafrooz V, Yazdimamaghani M, Vashaee D, Tayebi L. Multilayer bioactive glass/zirconium titanate thin films in bone tissue engineering and regenerative dentistry. Int J Nanomed. 2013;8:1665.
8. Tahmasbi Rad A, Ali N, Kotturi HSR, Yazdimamaghani M, Smay J, Vashaee D, et al. Conducting scaffolds for liver tissue engineering. J Biomed Mater Res A. 2014;102(11):4169–81.
9. Shahini A, Yazdimamaghani M, Walker K, Eastman M, Hatami-Marbini H, Smith B, et al. 3D conductive nanocomposite scaffold for bone tissue engineering. Int J Nanomed. 2014;9:167–81.
10. Kotwal A, Schmidt CE. Electrical stimulation alters protein adsorption and nerve cell interactions with electrically conducting biomaterials. Biomaterials. 2001;22:1055–64.
11. Bolin MH, Svennersten K, Wang XJ, Chronakis IS, Richter-Dahlfors A, Jager EWH, et al. Nano-fiber scaffold electrodes based on PEDOT for cell stimulation. Sens Actuator B-Chem. 2009;142:451–6.
12. Guimard NK, Gomez N, Schmidt CE. Conducting polymers in biomedical engineering. Prog Polym Sci. 2007;32:876–921.
13. Miklavčič D, Pavšelj N, Hart FX. Electric properties of tissues. Wiley encyclopedia of biomedical engineering; 2006.
14. Richardson-Burns SM, Hendricks JL, Foster B, Povlich LK, Kim D-H, Martin DC. Polymerization of the conducting polymer poly(3,4-ethylenedioxythiophene)(PEDOT) around living neural cells. Biomaterials. 2007;28:1539–52.
15. Luo S-C, Mohamed Ali E, Tansil NC, Yu H-h, Gao S, Kantchev EA, et al. Poly(3,4-ethylenedioxythiophene)(PEDOT) nanobiointerfaces: thin, ultrasmooth, and functionalized PEDOT films with in vitro and in vivo biocompatibility. Langmuir. 2008;24:8071–7.
16. Karagkiozaki V, Karagiannidis P, Gioti M, Kavatzikidou P, Georgiou D, Georgaraki E, et al. Bioelectronics meets nanomedicine for cardiovascular implants: PEDOT-based nanocoatings for tissue regeneration. Biochim Biophys Acta. 2013;1830:4294–304.
17. Kim DR, Abidian M, Martin D. Synthesis and characterization of conducting polymers grown in hydrogels for neural applications. In: Proceedings of the symposium on architecture and application of biomaterials and biomolecular materials, Boston, MA, 2003. p. 1–4.
18. Xiao X, Liu R, Liu F, Zheng X, Zhu D. Effect of poly(sodium 4-styrene-sulfonate) on the crystal growth of hydroxyapatite prepared by hydrothermal method. Mater Chem Phys. 2010;120:603–7.
19. Crispin X, Marciniak S, Osikowicz W, Zotti G, Van der Gon AWD, Louwet F, et al. Conductivity, morphology, interfacial chemistry, and stability of poly(3,4-ethylene dioxythiophene)-poly(styrene sulfonate): a photoelectron spectroscopy study. J Polym Sci Pt B-Polym Phys. 2003;41:2561–83.
20. Friedel B, Keivanidis PE, Brenner TJK, Abrusci A, McNeill CR, Friend RH, et al. Effects of layer thickness and annealing of PEDOT:PSS layers in organic photodetectors. Macromolecules. 2009;42:6741–7.
21. Hwang J, Amy F, Kahn A. Spectroscopic study on sputtered PEDOT center dot PSS: role of surface PSS layer. Org Electron. 2006;7:387–96.
22. Choi YS, Hong SR, Lee YM, Song KW, Park MH, Nam YS. Study on gelatin-containing artificial skin: I. Preparation and characteristics of novel gelatin-alginate sponge. Biomaterials 1999;20:409–17.
23. Ghasemi-Mobarakeh L, Prabhakaran MP, Morshed M, Nasr-Esfahani M-H, Ramakrishna S. Electrospun poly(ε-caprolactone)/gelatin nanofibrous scaffolds for nerve tissue engineering. Biomaterials. 2008;29:4532–9.
24. Yazdimamaghani M, Vashaee D, Assefa S, Shabrangharehdasht M, Rad AT, Eastman MA, et al. Green synthesis of a new gelatin-based antimicrobial scaffold for tissue engineering. Mater Sci Eng C. 2014;39:235–44.
25. Jones JR. Review of bioactive glass: from Hench to hybrids. Acta Biomater. 2013;9:4457–86.
26. Yazdimamaghani M, Razavi M, Vashaee D, Pothineni VR, Rajadas J, Tayebi L. Significant degradability enhancement in multilayer coating of polycaprolactone-bioactive glass/gelatin-

bioactive glass on magnesium scaffold for tissue engineering applications. Appl Surf Sci. 2015;338:137–45.
27. Kokubo T, Takadama H. How useful is SBF in predicting in vivo bone bioactivity? Biomaterials. 2006;27:2907–15.
28. Jones JR, Ehrenfried LM, Hench LL. Optimising bioactive glass scaffolds for bone tissue engineering. Biomaterials. 2006;27:964–73.
29. Fassina L, Saino E, Sbarra MS, Visai L, De Angelis MGC, Magenes G, et al. In vitro electromagnetically stimulated SAOS-2 osteoblasts inside porous hydroxyapatite. J Biomed Mater Res A. 2010;93:1272–9.
30. Sun S, Titushkin I, Cho M. Regulation of mesenchymal stem cell adhesion and orientation in 3D collagen scaffold by electrical stimulus. Bioelectrochemistry. 2006;69:133–41.
31. Lee K, Park M, Kim H, Lim Y, Chun H, Kim H, et al. Ceramic bioactivity: progresses, challenges and perspectives. Biomed Mater. 2006;1:R31.
32. Kim H-M. Ceramic bioactivity and related biomimetic strategy. Curr Opin Solid State Mater Sci. 2003;7:289–99.
33. Hench LL, Xynos ID, Polak JM. Bioactive glasses for in situ tissue regeneration. J Biomater Sci Polym Ed. 2004;15:543–62.
34. Hronik-Tupaj M, Kaplan DL. A review of the responses of two- and three-dimensional engineered tissues to electric fields. Tissue Eng B: Rev. 2012;18:167–80.
35. Darendeliler MA, Darendeliler A, Sinclair PM. Effects of static magnetic and pulsed electromagnetic fields on bone healing. Int J Adult Orthod Orthognath Surg. 1997;12:43–53.
36. Shupak NM, Prato FS, Thomas AW. Therapeutic uses of pulsed magnetic-field exposure, a review. Radio Sci Bull 2003;307:9–32.
37. Meng SY, Zhang Z, Rouabhia M. Accelerated osteoblast mineralization on a conductive substrate by multiple electrical stimulation. J Bone Miner Metab. 2011;29:535–44.
38. Ryaby JT. Clinical effects of electromagnetic and electric fields on fracture healing. Clin Orthop Relat Res. 1998;355:S205–15.
39. Shiyun Meng MR, Ze Zhang. Electrical stimulation in tissue regeneration. INTECH Open Access Publisher, 2011.
40. Tabrah F, Hoffmeier M, Gilbert F, Batkin S, Bassett CAL. Bone-density changes in osteoporosis-prone women exposed to pulsed electromagnetic-fields (PEMFS). J Bone Miner Res. 1990;5:437–42.
41. Tandon N, Goh B, Marsano A, Chao P-H, Montouri-Sorrentino C, Gimble J, et al. Alignment and elongation of human adipose-derived stem cells in response to direct-current electrical stimulation. Engineering in medicine and biology society, 2009 EMBC 2009 annual international conference of the IEEE: IEEE; 2009. p. 6517–21.
42. Li XF, Kolega J. Effects of direct current electric fields on cell migration and actin filament distribution in bovine vascular endothelial cells. J Vasc Res. 2002;39:391–404.